Interaction of Helium Ion Beam with Argon Gas and Plasma

Atsushi OKAMOTO, Takehiro ISONO, Takashi KOBUCHI, Sumio KITAJIMA and Mamiko SASAO

Department of Quantum Science and Energy Engineering, Tohoku University, Sendai 980-8579 Japan

(Received: 1 September 2008 / Accepted: 20 March 2009)

A helium ion beam is extracted and is injected into an argon gas and a plasma in a linear device in terms of experimental study of interaction between energetic ions in divertor plasmas and gases for radiator. The beam with the energy of 0-10 keV passing through the argon gas is attenuated by charge-exchange and elastic collisions with increasing the filling gas pressure. The electron temperature (~ 10 eV) and density ($\sim 10^7$ cm^{-3}) of a bulk plasma degrade under the ion beam in some conditions. A beam-produced plasma is also observed. Although mechanism of the degradation is unresolved, the argon gas in the divertor is expected to moderate the momentum flux of energetic ion.

Keywords: Ion Beam, Beam Injection, Beam-Plasma Interaction, Divertor Plasma

1. Introduction

Interactions between energetic particles and plasmas are an interesting topic in the research field of the magnetically confined plasma as well as in that of the basic plasma physics. Energetic particle flux into the divertor is considered to change the balance of atomic processes in the detached divertor plasma[1]. In order to reduce heat flux onto the divertor plate, radiative cooling of the divertor plasma is performed prior to its volumetric recombination. Therefore the radiator, puffed noble gases, also interacts with the energetic particle; efficiency of the radiative cooling is potentially affected. It is important to understand behavior of the radiator against the energetic particle as well as to understand mechanism of plasma detachment and the recombination processes. While the energetic particle originates from a pedestal plasma and its energy reaches several keV in ITER[2], puffed argon is a candidate of the radiator. Thus, interaction between several-keV ion and partially ionized argon plasma is a significant process in the divertor region.

In order to investigate such research fields, a simple experimental apparatus with an ion beam is useful to complement results of real divertor in magnetic confinement devices. We have launched an experimental study on the beam-plasma interaction using a linear plasma device with an ion source. In this paper, development of ion beam injection system applicable to the linear plasma device is described. Then interaction of a helium-ion beam with argon gas and that with plasma are presented. Significant beam attenuation due to atomic interactions is indicated, while a plasma modified in some conditions is shown. The linear plasma device, named DT-ALPHA, has been constructed and has been used for experiment since 2007 JPY[3], while an ion source has been installed in DT-ALPHA since 2008. Those are described in Sec. 2. Experiments on plasma production and ion beam extraction are explained in Sec. 3, where results of the ion beam injection into an argon gas and an argon plasma are also shown, followed by discussion in Sec. 4.

author's e-mail: atsushi.okamoto@qse.tohoku.ac.jp

2. Experimental Setup

2.1 DT-ALPHA device

The experiments were performed in a linear plasma device equipped with an ion source. The former was originally designed as a "Diagnostic Tool Assisted by Linear Plasma device for Helium Atom beam (DT-ALPHA)"[3]. A schematic of the experimental setup is shown in Fig. 1. The vacuum chamber consists of an ion source, a differential pumping chamber equipped with a Faraday cup, a quartz pipe (0.4 m in length) coupling an antenna to a plasma, and a main chamber (1.1 m in length) made of stainless steel. An aperture with an inner diameter of 10 mm made of stainless steel is equipped at the entrance of the quartz pipe, $z = 0.49$ m, where z is the distance from the ion source. The aperture is connected to the ground through a 1-kΩ resistor. An end-plate assembly, which consists of the center plate and four azimuthally segmented plates, is installed at the end of the main chamber, $z = 2.02$ m. All the end-plates are made of stainless steel and are connected to the ground through a 1-kΩ resistor.

A magnetic field, which is a mirror configuration with the mirror ratio $R_{\mathrm{M}} = 1.4$ and the mirror throats located at $z = 0.60, 1.65$ m, is applied along the axial direction. Magnetic field intensity is $B = 0.11$ T at the center ($z = 1.17$ m). A so-called Nagoya type III antenna[4] ($l = 0.15$ m) is used in the present experiment, which is connected to a 13.56 MHz radio frequency (RF) oscillator through a matching cir-

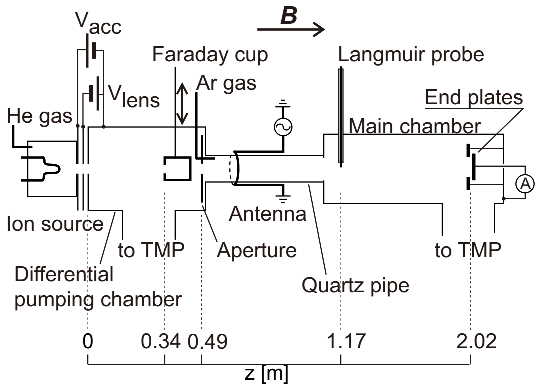

Fig. 1 Schematic of the experimental setup.

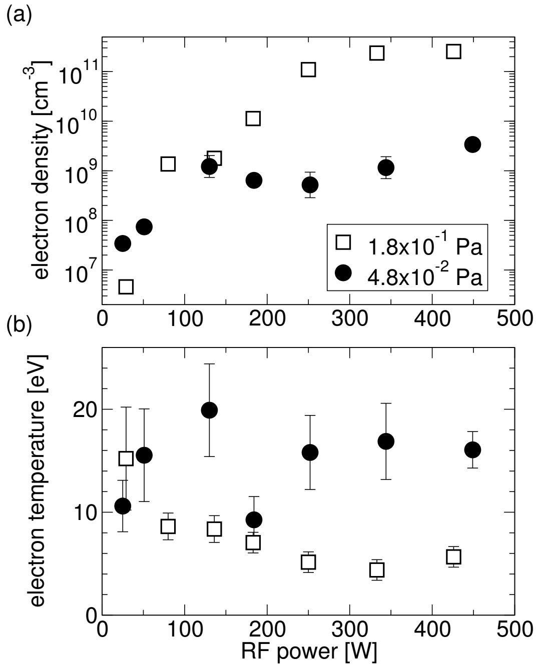

Fig. 2 RF power dependence of electron density and temperature of an argon plasma measured in two different pressures.

cuit. An argon plasma is produced under the condition of the RF power up to 500 W and with working pressure of 0.04-0.2 Pa. Blue plasmas are partially produced near the antenna, which imply strong emission of ArII[5] and is regarded as a marker of helicon discharge[6, 7, 8, 9].

Plasma parameters are evaluated using the current (I)- voltage (V) characteristics of a single Langmuir probe installed at $z = 1.17$ m. The probe made of a molybdenum wire ($l \simeq 1.2$mm, $d \simeq 0.6$mm) is biased in a range of -120 V to 70 V.

2.2 Ion Source

A multicusp ion source is installed in the end of the quartz pipe through a differential pumping chamber. The ion source is made of copper and has 80 mm diameter and 90 mm long inside volume[10, 11]. Permanent magnets attached at the wall form line cusp magnetic field for plasma confinement. A 0.2 standard cubic centimeter per minute (SCCM) of helium gas is injected into the ion source chamber. Then the pressure of the chamber is estimated to be 0.1 Pa. A hot tungsten filament serves as the cathode of an arc discharge. A constant-voltage ($V_{\mathrm{arc}} = 80$ V) power-supply is used for the arc discharge; up to $P_{\mathrm{arc}} = 130$ W ($I_{\mathrm{arc}} = 1.6$ A) of arc power are injected into the ion source.

Helium ion beams extracted from an 6 mm diameter extraction hole are injected into target plasmas. The extraction system consists of three electrodes, the plasma electrode, the lens electrode, and the ground electrode. The ion source chamber is connected to a potential of the acceleration power supply, V_{acc}, which varies over 0-10 kV. The voltage of the lens electrode, which is negative $-V_{\mathrm{lens}}$ with respect to the ground electrode, is adjusted to the optimum beam current. The ion beam current is measured by both the movable Faraday cup located at $z = 0.34$ m and the center end-plate.

3. Experimental Result

3.1 Plasma Parameter without Beams

RF power dependence of the electron density and temperature are shown in Fig. 2. The open square represents the result obtained in a high working-gas pressure (1.8×10^{-1} Pa) experiment. The electron density reaches $3 \times 10^{11}\mathrm{cm}^{-3}$ in the RF power $P_{\mathrm{RF}} >$ 300 W region. The electron temperature is about 15 eV for $P_{\mathrm{RF}} < 50$ W and is gradually decreases with the density increasing.

In the low pressure (4.8×10^{-2} Pa) operation, the density increases up to $3 \times 10^{9}\mathrm{cm}^{-3}$ with the RF power, while the electron temperature is about 10-20 eV. These densities are two or three orders lower than that obtained in the high pressure operation. However, in order to sustain stable arc discharge in the ion source, the lower gas pressure condition was selected in the present experiment as a target plasma of the beam injection.

3.2 Ion Beam Extraction

Typical radial distribution of the beam current density measured by the Faraday cup is shown in Fig. 3(a). The condition of the beam extraction are arc current $I_{\mathrm{arc}} = 1.1$ A, acceleration voltage $V_{\mathrm{acc}} = 4.5$ kV, and lens voltage $V_{\mathrm{lens}} = 0.25$ kV. Total beam current and the half width at 1/e times the maximum in the beam profile, which are obtained by deconvolution of the instrumental function, are 0.52 mA and 0.68 cm, respectively.

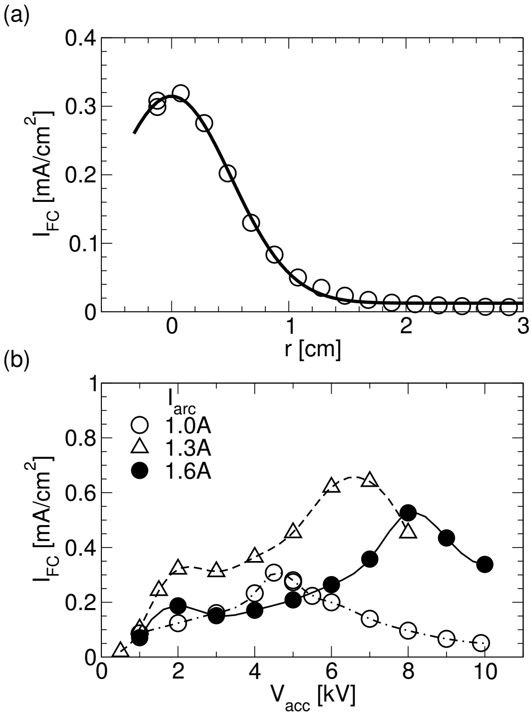

Fig. 3 (a) Radial distribution of beam current density measured under the conditions of $V_{\mathrm{arc}} = 80$ V, $I_{\mathrm{arc}} = 1.1$ A, $V_{\mathrm{acc}} = 4.5$ kV, and $V_{\mathrm{lens}} = 0.25$ kV. (b) Acceleration voltage dependence of beam current density under the condition of $V_{\mathrm{arc}} = 80$ V. The lenz voltage is adjusted to maximize the beam current density for each acceleration voltage.

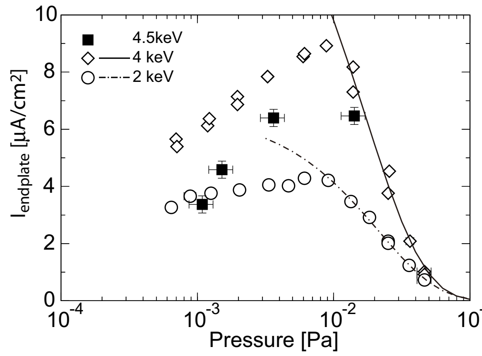

Fig. 4 End-plate current-density vs. filling gas pressure. Ion beams are extracted with various acceleration voltage. Solid line represents $I_{\mathrm{endplate}} = I_0 \exp(-\alpha p)$ with $\alpha = 58.5\ \mathrm{Pa}^{-1}, I_0 = 17.6\ \mu\mathrm{A/cm}^2$ for $V_{\mathrm{acc}} = 4.0$ kV, dash-dotted line with $\alpha = 46.4\ \mathrm{Pa}^{-1}, I_0 = 6.58\ \mu\mathrm{A/cm}^2$ for $V_{\mathrm{acc}} = 2.0$ kV, respectively.

Acceleration voltage dependence of the beam current density is shown in Fig. 3(b). Optimized acceleration voltages for each arc current exist, in which the current density has local maxima. While one maximum locates at $V_{\mathrm{acc}} = 4.5$ kV for $I_{\mathrm{arc}} = 1.0$ A, two local maxima exist for $I_{\mathrm{arc}} \geq 1.3$ A. Ones observed around $V_{\mathrm{acc}} = 6 - 8$ kV for $I_{\mathrm{arc}} \geq 1.3$ A are a series of that observed at $V_{\mathrm{acc}} = 4.5$ kV for $I_{\mathrm{arc}} = 1.0$ A. The optimized acceleration voltage for these increases with the arc current. Other local maxima appear around $V_{\mathrm{acc}} = 2.0$ kV, where the extraction voltage ($V_{\mathrm{ext}} \equiv V_{\mathrm{acc}} + V_{\mathrm{lens}}$) is a little smaller than that optimized for $V_{\mathrm{acc}} = 4 - 8$ kV, suggesting that a beam optics suitable for the low energy beam has a shallow meniscus at the plasma electrode. Maximum current density of $0.64\mathrm{mA/cm}^2$ is extracted when $V_{\mathrm{acc}} = 7.0$ kV and $I_{\mathrm{arc}} = 1.3$ A.

3.3 Effect of Beam Injection

Ion beam injection into an argon gas was performed in order to investigate beam attenuation in the argon gas and to obtain experimental window for beam injection into an argon plasma. The center end-plate was used to monitor the beam current passing through the chamber of DT-ALPHA. Current density of the end-plate is proportional to the beam current density. Figure 4 shows filling gas pressure dependence of the end-plate current. The current density gradually increases with the filling gas pressure and saturates around 0.01 Pa. Because the space charge of the ion beam is canceled by weakly ionized ambient gas, the current density measured with the gas is larger than that without gas.

On the other hand, the current density decreases in the higher pressure region. Curves indicating an exponential function, $I_{\mathrm{endplate}} = I_0 \exp(-\alpha p)$, agree with the data within the parameter $\alpha = 50 \pm 10\ \mathrm{Pa}^{-1}$ in the both beam energy. The result shows that the ion beams are attenuated by interactions with weak energy-dependence. Then the effective cross-section, $\sigma = \alpha p/nl = 1 \times 10^{-15}\mathrm{cm}^2$ is obtained, where nl represents the line integrated density of the argon gas. Since both the cross-section of charge-exchange reaction[12] and that of elastic scattering[13] are order of $10^{-15}\mathrm{cm}^2$, the beam attenuation observed in Fig. 4 is considered to be caused by those atomic processes. Under the working gas pressure for plasma production, $p = 4.8 \times 10^{-2}$ Pa, the ion beam sufficiently interact with argon gas and is attenuated.

Effect of ion beam injection on target plasma parameter is investigated. Up to 8 keV of helium ion beams are injected into various densities of argon plasmas. Figure 5(a) shows the electron density, which increases with the RF power. Ion beam injection decreases electron density to some extent, while the electron temperature shown in Fig. 5(b) also decreases by the beam injection. In these experiments, a matching condition was unchanged against the beam injection. However the changes of the plasma param-

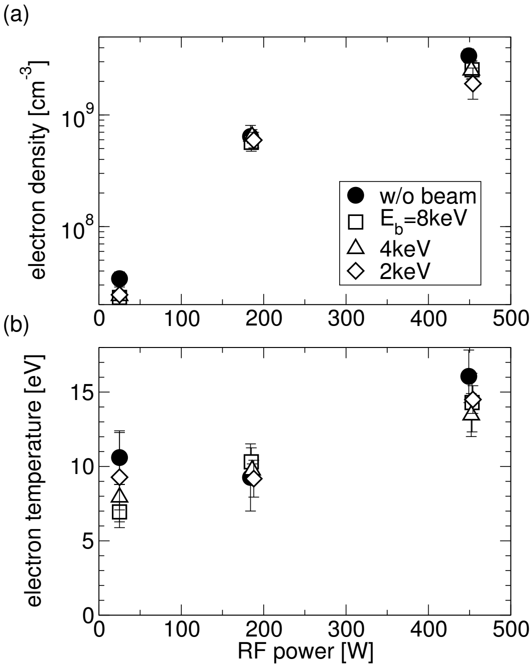

Fig. 5 RF power dependence of electron density and temperature of an argon plasma with various energy of ion beam injection.

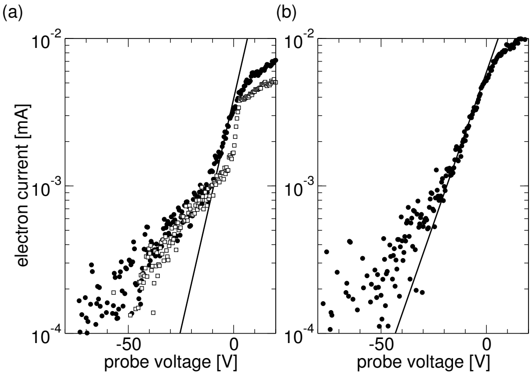

Fig. 6 (a) Electron current characteristic curve with 8 keV-He^+ beam injection. Filled circle represents that obtained with an Ar plasma produced by $P_{\rm RF}$ = 25 W. Open square represents without plasma. Solid line shows a slope corresponding to the bulk temperature. (b) the same as (a) but without an ion beam.

eter are within the order of error and no significant change is observed for a middle density ($P_{\rm RF} \simeq 200$ W) plasma. Further investigation is required for quantitative discussion.

In some beam injections, a tail component is observed in the probe characteristic curve. Filled circle in Fig. 6(a) corresponds to a result with beam injection, where the bulk temperature is $T_{\rm e} = 7$ eV and a tail component has a slope of 30 eV. The tail component also emerges only with the ion beam injection as indicated by a probe characteristic curve (open square). On the other hand, the same plasma production but no beam injection, clear tail component is not observed as shown in Fig. 6(b). The presence of the tail component implies that low density plasma is produced by the ion beam but is not fully thermalized.

4. Discussion

Between the charge-exchange and the elastic collisions, which interaction dominates the beam attenuation is an interest problem. However it is also a difficult problem, because accurate cross-sections of those collisions are insufficient especially in the energy range 1-10 keV. The cross-section of the elastic collision has, in general, a monotonic dependence $\sigma_{\rm el} \sim E^{-2}$, while that of the charge-exchange $\sigma_{\rm CX}(E)$ has a peak at $E = 20 - 30$ keV[12]; competition between the decreasing function $\sigma_{\rm el}(E)$ and the increasing function $\sigma_{\rm CX}(E)$ is expected in several keV.

The charge-exchange process neutralizes the energetic ions resulting in reduction of momentum flux along the magnetic field in the divertor region. Thus the argon gas puffed into the divertor is expected to moderate the momentum flux as well as to reduce electron energy by radiation.

Mechanism of the electron temperature and density degradation under ion beam injection is unresolved. Precise and wide-parameter measurements including beam detection in a plasma and some optical methods will be requreid for detailed discussion. Fluctuations might be a key in terms of the wave-particle interactions, which excite instabilities affecting the plasma.

In summary, a several-keV of helium ion beam is injected into an argon gas and a plasma. The beam passing through the argon gas is attenuated by charge-exchange and elastic collisions. The bulk plasma degrade under ion beam in some condition. However why the bulk plasma is affected by the beam and the beam-produced plasma remains our future work. The argon gas in the divertor is expected to moderate the momentum flux of energetic ion.

Acknowledgements

This work was partly supported by the Ministry of Education, Culture, Sports, Science and Technology of Japan (MEXT) Grant-in-Aid for "Priority area of Advanced Burning Plasma Diagnostics" (16082201). Authors acknowledges for the support for young scientists by the school of engineering in Tohoku University.

[1] N. Ohno, D. Nishijima, S. Takamura, Y. Uesugi, M. Motoyama, N. Hattori, H. Arakawa, N. Ezumi, S. Krasheninnikov, A. Pigarov, U. Wenzel, *Nucl. Fusion* **41**, 1055 (2001).

[2] A. Loarte, B. Lipschultz, A.S. Kukushkin, *et al.*, *Nucl. Fusion* **47**, S203 (2007).
[3] A. Okamoto, K. Iwazaki, T. Isono, T. Kobuchi, S. Kitajima, and M. Sasao, *Plasma Fusion Res.* **3**, 059 (2008).
[4] T. Watari, T. Hatori, R. Kumazawa, S. Hidekuma, T. Aoki, T. Kawamoto, M. Inutake, S. Hiroe, A. Nishizawa, K. Adati, T. Sato, T. Watanabe, H. Obayashi, and K. Takayama, *Phys. Fluids* **21**, 2076 (1978).
[5] R.W. Boswell, *Plasma Phys. Control. Fusion* **26**, 1147 (1984).
[6] T. Shoji, Y. Sakawa, S. Nakazawa, K. Kadota, and T. Sato, *Plasma Sources Sci. Technol.* **2**, 5 (1993).
[7] S. Shinohara, Y. Miyauchi, and Y. Kawai, *Plasma Phys. Control. Fusion* **37**, 1015 (1995).
[8] F.F. Chen, *Phys. Plasmas* **3**, 1783 (1996).
[9] Y. Sakawa, T. Takino, and T. Shoji, *Phys. Plasmas* **6**, 4759 (1999).
[10] K. Shinto, H. Sugawara, M. Takenaga, S. Takeuchi, N. Tanaka, A. Okamoto, S. Kitajima, M. Sasao, M. Nishiura, M. Wada, *Rev. Sci. Instrum.* **77**, 03B512 (2006).
[11] H. Sugawara, K. Shinto, N. Tanaka, S. Takeuchi, M. Kikuchi, A. Okamoto, S. Kitajima, M. Sasao, M. Wada, *Rev. Sci. Instrum.* **79**, 02B708 (2008).
[12] M.E. Rudd, T.V. Goffe, A. Itoh, R.D. DuBois *Phys. Rev. A* **32**, 829 (1985).
[13] S. Takeuchi, M. Sasao, H. Sugawara, N. Tanaka, M. Kisaki, A. Okamoto, K. Shinto, S. Kitajima, M. Nishiura, M. Wada, *Rev. Sci. Instrum.* **79**, 02A509 (2008).